International Journal of Innovative
Computing, Information and Control
Volume **16**, Number **3**, June **2020**

 ISSN 1349-4198
pp. 1109–1116

SWITCHED CAPACITOR-BASED HIGH VOLTAGE MULTIPLIER WITH 220V@50HZ INPUT FOR GENERATING UNDERWATER SHOCKWAVES

Anurak Jaiwanglok[1], Kei Eguchi[2] and Amphawan Julsereewong[1]

[1]Faculty of Engineering
King Mongkut's Institute of Technology Ladkrabang
Ladkrabang, Bangkok 10520, Thailand
anurak.jai@hotmail.com; amphawan.ju@kmitl.ac.th

[2]Department of Information Electronics
Fukuoka Institute of Technology
3-30-1 Wajiro-higashi, Higashi-ku, Fukuoka 811-0295, Japan
eguti@fit.ac.jp

Received December 2019; revised March 2020

Abstract. *Non-thermal food processing using underwater shockwaves is a cost-effective technology for preserving food items with minimal impacts on their nutritious property. In order to generate underwater shockwaves, a high voltage multiplier is the major element for system hardware implementation. To support the 220V and 50Hz AC input for generating 3.7kV DC output, this paper presents the high voltage multiplier based on switched capacitor technique. The proposed circuit consists of three main components, which are AC-DC rectifier, level shift driver, and parallel-connected voltage multiplier circuit. The theoretical relationship analysis utilizing a 4-terminal equivalent circuit is described for investigation of not only the output voltage but also the energy loss due to internal resistance and the power efficiency of the proposed high voltage multiplier. In addition, the operations of the proposed circuit are also simulated by using PSPICE program to confirm its workability.*

Keywords: AC-DC rectifier, High voltage multiplier, Non-thermal food processing, Switched capacitor, Underwater shockwave

1. **Introduction.** Generally, a thermal food processing for ensuring food safety often has unintended consequences for changing nutritional and sensorial properties of food items by overheating methods. To overcome this limitation, a non-thermal food processing becomes an alternative solution for preserving food products with minimal quality losses [1]. Food preservation using underwater shockwaves induced by gap discharge is one of low-heat generation approaches for implementing non-thermal food processing systems [2-4]. Recently, circuit realizations without magnetic components to generate underwater shockwaves for cost-effective non-thermal food processing have been presented [5-8]. These shockwave generations are based on the use of high voltage multipliers designed by switched capacitor technique to create high DC output voltage in range of 3.5-4.0kV. A digitally controlled voltage multiplier that consists of full waveform rectifier, 2-phase clock pulse generator, positive voltage multiplier block, and negative voltage multiplier block has been proposed [5]. Its DC output voltage at the last stage can be obtained by sum of the outputs of positive and negative multiplier blocks, which are connected together in bipolar structure. To enhance voltage efficiency of the bipolar high voltage multiplier, a 2-phase clock pulse generator with through-current preventing circuit has

DOI: 10.24507/ijicic.16.03.1109

been described [6]. In addition, using 4-phase clock pulse generator formed by level shift drivers to control operations of the bipolar high voltage multiplier has also been proposed [7]. Based on this proposed control technique, the high voltage multiplier employing level shift drivers can generate the DC output voltage more than 3.5kV at high speed. Alternatively, a high voltage multiplier using inductor-less AC-AC converters to replace full waveform rectifier for minimizing circuit components has been introduced [8]. However, the high voltage multiplier without the use of full waveform rectifier provides slow response speed, which is not appropriate for high-speed non-thermal food processing using underwater shockwaves, because the time period to operate non-thermal food processing depends mainly on the operation speed of high voltage multiplier [9,10]. Nevertheless, the switched capacitor-based high voltage multipliers proposed in [5-7] and [8] are designed for applying 100V@60Hz and 100V@50Hz AC inputs, respectively. In order to be more applicable for non-thermal food processing utilizing underwater shockwaves, the high voltage multiplier should operate with other AC voltage inputs. This paper aims to propose a circuit realization technique for high voltage generator that is suitable for 220V@50Hz AC input to generate 3.7kV DC output. The characteristics of the proposed multiplier are theoretically analyzed, and its effectiveness is verified through PSPICE simulation results.

The remainder of this article is organized as follows. The realization concept and circuit description of the proposed high voltage multiplier are detailed in Section 2. The theoretical analysis and simulation results are shown in Section 3 and Section 4, respectively. The conclusions and possible future work are lastly discussed in Section 5.

2. Proposed High Voltage Multiplier.

2.1. Realization concept. Figure 1 displays a conceptual block diagram for realizing the proposed high voltage multiplier, which comprises three main sections: AC-DC rectifier, level shift driver, and parallel-connected voltage multiplier circuit. The proposed circuit realization is based on modifications from the bipolar voltage multiplier controlled by high speed driver circuit [7] and the conventional Cockcroft-Walton voltage multipliers [11,12] for applying 220V@50Hz input signal. In the 1st Section, the positive AC input is converted into DC signal and then this positive DC signal is multiplied by 2, while the negative AC input is converted into the negative DC signal. In the 2nd Section, the level shift driver switches the voltage according to clock pulses from the first section to the last

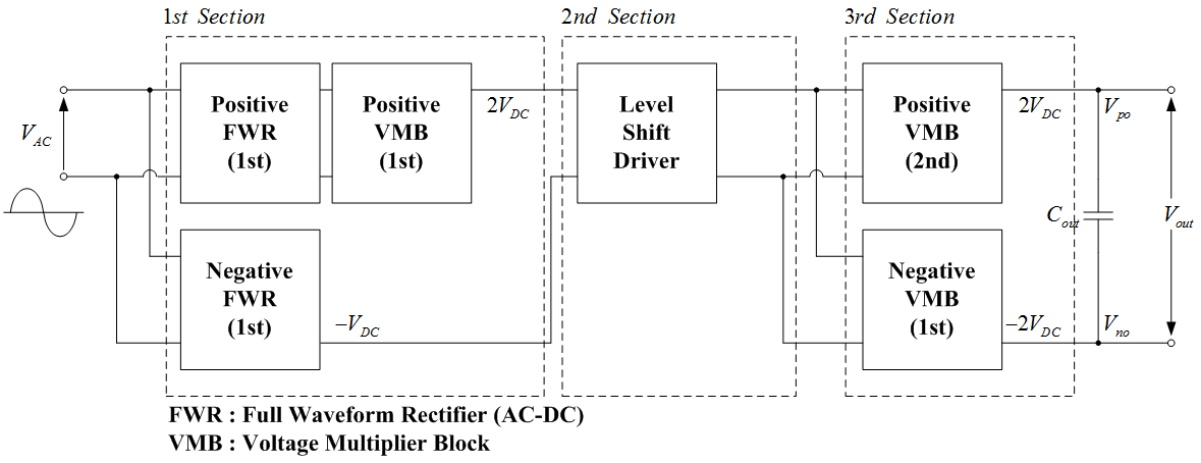

FIGURE 1. Block diagram for realizing the proposed high voltage multiplier

section. In the 3rd Section, the positive and negative voltage multiplier blocks (VMBs) are used to multiply the positive and negative DC signals by 2 and −2, respectively. Based on the parallel connection of these two VMBs, the step-up gain of 12 can be obtained.

2.2. **Circuit description.** Based on the concept of Figure 1, the proposed high voltage multiplier can be illustrated as Figure 2, which includes 12 capacitors, 18 diodes, and 4 switches. The parameters V_{in}, V_{po}, V_{no}, and V_{out} are referred as input voltage, positive output voltage, negative output voltage, and output voltage, respectively. The relation between V_{po}, V_{no}, and V_{out} can be stated as

$$V_{out} = V_{po} - V_{no} \tag{1}$$

The capacitors C_{pk} $(k = 1, 2, 3)$, C_{nl} $(l = 1)$ and C_{1pq}, C_{2pq} $(q = 1, 2)$, C_{1nr}, C_{2nr} $(r = 1, 2)$ are referred to the capacitors connected in the 1st Section and the 3rd Section, respectively. The switches S_x $(x = 1, 2, 3, 4)$ are referred to the switches connected in the 2nd Section. The clock pulses for the level shift driver can be expressed as

$$T = T_1 + T_2, \quad T_1 = DT \text{ and } T_2 = (1 - D)T \tag{2}$$

where T is the clock time period, T_1 is the time period for closing the switches S_1 and S_4, T_2 is the time period for closing the switches S_2 and S_3, and D is the duty cycle of 50%.

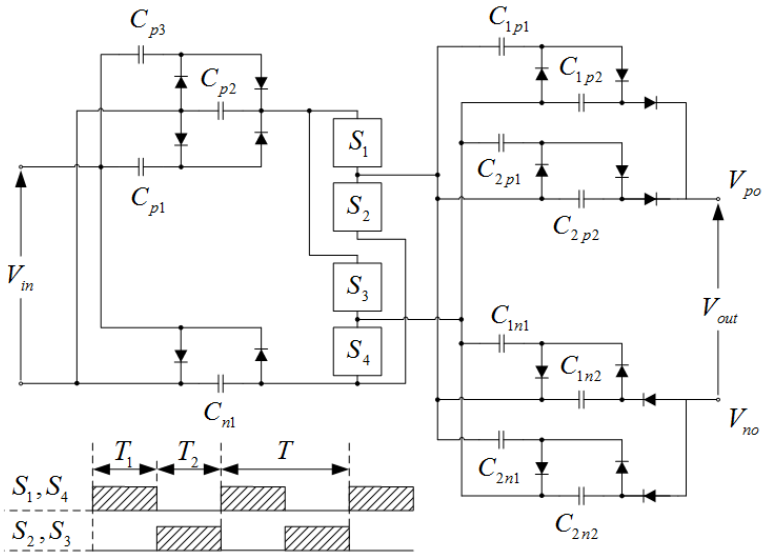

FIGURE 2. Proposed high voltage multiplier

3. **Theoretical Analysis.** The characteristics of the proposed high voltage multiplier in terms of output voltage, energy loss due to internal resistance and power efficiency are interested. In order to analyze the interested characteristics, a 4-terminal equivalent circuit of the proposed multiplier is shown in Figure 3. The parameters referred in this equivalent circuit are that M, R_{SC}, and R_L denote the turn ratio of ideal transformer, the internal resistance, and the output load, respectively. It should be noted that three analysis conditions are assumed. The first condition is that the device latencies are not considered in the analysis. The second condition is that the time constant of the proposed circuit must be greater than the period of the clock pulse. The last condition is that the input signal is represented as the rectangular waveform.

The instantaneous equivalent circuits in steady state of *State-*T_{r1}, *State-*T_{r2}, *State-*T_{m1}, and *State-*T_{m2} are depicted in Figure 4. The referred parameters are that R_d is

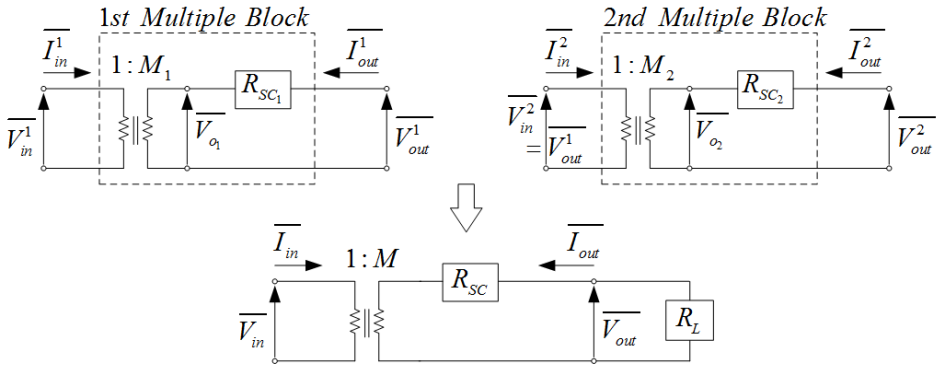

FIGURE 3. 4-terminal equivalent circuit for theoretical analysis

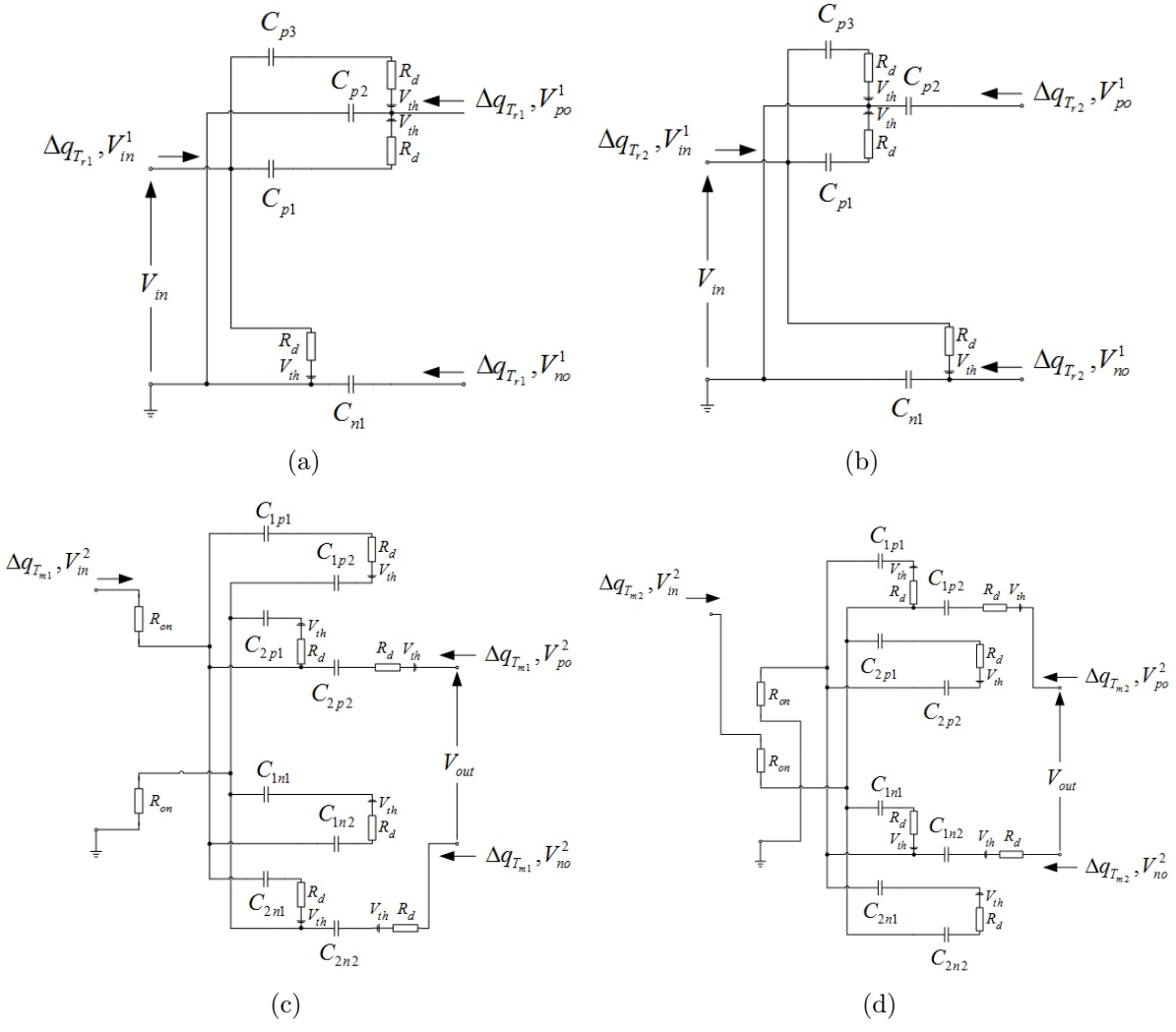

FIGURE 4. Instantaneous equivalent circuits during steady state: (a) *State-*T_{r1}, (b) *State-*T_{r2}, (c) *State-*T_{m1}, and (d) *State-*T_{m2}

the diode 'ON' resistance, V_{th} is the diode threshold voltage, and R_{on} is the switch 'ON' resistance. From Figures 4(a) and 4(b), the differential values of electric charges in C_{pk} $(k = 1, 2, 3)$ and C_{nl} $(l = 1)$ can be explained as

$$\Delta q^{pk}_{T_{r1}} + \Delta q^{pk}_{T_{r2}} = 0 \text{ and } \Delta q^{nl}_{T_{r1}} + \Delta q^{nl}_{T_{r2}} = 0 \tag{3}$$

where

$$T_r = \sum_{i=1}^{2} T_{ri} = T_{r1} + T_{r2} \text{ and } T_{r1} = T_{r2} = \frac{T_r}{2}$$

The parameters referred in (3) are that $\Delta q_{T_{ri}}^{pk}$ is the differential value of electric charges in C_{pk} of the positive voltage multiplier, and $\Delta q_{T_{ri}}^{nl}$ is the differential value of electric charges in C_{nl} of the negative voltage multiplier. Moreover, the time period T_r depends on the frequency of the AC input voltage V_{in}. Therefore, the relationship of the electric charges can be given by

$$\Delta q_{T_{ri}}^{p1} = \Delta q_{T_{ri}}^{p3} \tag{4}$$

From Figures 4(a) and 4(b), the differential values of electric charges can be stated as

$$\begin{aligned}
\textit{State-}T_{r1} \quad & \Delta q_{T_{r1}}, V_{in}^1 = \Delta q_{T_{r1}}^{p1} + \Delta q_{T_{r1}}^{p3} + \Delta q_{T_{r1}}^{n1} \\
& \Delta q_{T_{r1}}, V_{po}^1 = -\Delta q_{T_{r1}}^{p1} + \Delta q_{T_{r1}}^{p2} - \Delta q_{T_{r1}}^{p3} \\
\text{and} \quad & \Delta q_{T_{r1}}, V_{no}^1 = \Delta q_{T_{r1}}^{n1} \qquad (5) \\
\textit{State-}T_{r2} \quad & \Delta q_{T_{r2}}, V_{in}^1 = -\Delta q_{T_{r2}}^{p1} - \Delta q_{T_{r2}}^{p3} + \Delta q_{T_{r2}}^{n1} - \Delta q_{T_{r2}}, V_{no}^1 \\
\text{and} \quad & \Delta q_{T_{r2}}, V_{po}^1 = \Delta q_{T_{r2}}^{p2} \qquad (6)
\end{aligned}$$

The parameters referred in (5) and (6) are that $\Delta q_{T_{ri}}, V_{in}^1$, $\Delta q_{T_{ri}}, V_{po}^1$, and $\Delta q_{T_{ri}}, V_{no}^1$ denote the differential values of electric charges in the input voltage V_{in}^1, the output voltage of the positive voltage multiplier V_{po}^1, and the output voltage of the negative voltage multiplier V_{no}^1, respectively. Therefore, the turn ratio M of ideal transformer in Figure 3 can be obtained from the relationship of the input and output currents as follows:

$$\overline{I_{in}} = \frac{1}{T}\left(\sum_{i=1}^{2} \Delta q_{T_i,V_{in}}\right) = \frac{\Delta q_{V_{in}}}{T} \text{ and } \overline{I_{out}} = \frac{1}{T}\left(\sum_{i=1}^{2} \Delta q_{T_i,V_{out}}\right) = \frac{\Delta q_{V_{out}}}{T} \tag{7}$$

In (7), the total change of the input and output currents is equal to zero in the constant state, where $\Delta q_{V_{in}}$ and $\Delta q_{V_{out}}$ are the differential values of electric charges in the input and output voltages, respectively. Therefore, the relationship between the input and output currents by substituting (3)-(6) into (7) can be expressed as

$$\overline{I_{in}^1} = -3\overline{I_{out}^1} \text{ and } \overline{I_{out}^1} = \overline{I_{po}^1} = -\overline{I_{no}^1} \tag{8}$$

In (8), the turn ratio M_1 of Figure 3 is equal to 3 ($M_1 = 3$). From Figures 4(a) and 4(b), the value of the internal resistance R_{SC_1} can be explained in terms of the consumed energies $W_{T_{r1}}$ and $W_{T_{r2}}$ as follows.

$$W_{T_{r1}} = \frac{2R_d}{T_{r1}}\left(\Delta q_{T_{r1}}^{p2}\right)^2 + \frac{R_d}{T_{r1}}\left(\Delta q_{T_{r1}}^{n1}\right)^2 \tag{9}$$

$$W_{T_{r2}} = \frac{2R_d}{T_{r2}}\left(\Delta q_{T_{r2}}^{p2}\right)^2 + \frac{R_d}{T_{r2}}\left(\Delta q_{T_{r2}}^{n1}\right)^2 \tag{10}$$

Combining (9) and (10), the consumed energy in the time period T_r in the 1st Section can be given by

$$W_{T_r} = W_{T_{r1}} + W_{T_{r2}} = \frac{6R_d}{T_r}\left(\Delta q, V_{out}\right)^2 \tag{11}$$

In Figure 3, the consumed energy of the 4-terminal equivalent circuit can be written as

$$W_T = \left(\frac{\Delta q_{V_{out}}}{T}\right)^2 R_{SC} T \tag{12}$$

Therefore, the internal resistance in the 1st Section can solve from (11) and (12), which can be stated as

$$R_{SC_1} = 6R_d \tag{13}$$

For the 2nd Section shown in Figures 4(c) and 4(d), the differential values of electric charges in C_{1pq}, C_{2pq} $(q = 1, 2)$ and C_{1nr}, C_{2nr} $(r = 1, 2)$ can be written as

$$\begin{aligned} \Delta q_{T_{m1}}^{1pq} + \Delta q_{T_{m2}}^{1pq} = 0 \text{ and } \Delta q_{T_{m1}}^{2pq} + \Delta q_{T_{m2}}^{2pq} = 0 \\ \Delta q_{T_{m1}}^{1nr} + \Delta q_{T_{m2}}^{1nr} = 0 \text{ and } \Delta q_{T_{m1}}^{2nr} + \Delta q_{T_{m2}}^{2nr} = 0 \end{aligned} \tag{14}$$

where

$$T_m = \sum_{i=1}^{2} T_{mi} = T_{m1} + T_{m2} \text{ and } T_{m1} = T_{m2} = \frac{T_m}{2}$$

The parameters referred in (14) are that $\Delta q_{T_{mi}}^{1pq}$ and $\Delta q_{T_{mi}}^{2pq}$ are the differential values of electric charges in C_{1pq} and C_{2pq} of the positive voltage multiplier, $\Delta q_{T_{mi}}^{1nr}$ and $\Delta q_{T_{mi}}^{2nr}$ are the differential values of electric charges in C_{1nr} and C_{2nr} of the negative voltage multiplier. In addition, the time period T_m is dependent on the switching frequency of the level shift driver. Therefore, due to the symmetrical circuit structure, the relationship of the electric charges can be expressed as

$$\Delta q_{T_{m1}}^{1pq} = \Delta q_{T_{m2}}^{2pq}, \quad \Delta q_{T_{m1}}^{2pq} = \Delta q_{T_{m2}}^{1pq}, \quad \Delta q_{T_{m1}}^{1nr} = \Delta q_{T_{m2}}^{2nr} \text{ and } \Delta q_{T_{m1}}^{2nr} = \Delta q_{T_{m2}}^{1nr} \tag{15}$$

In Figures 4(c) and 4(d), the differential values of electric charges can be written as

$$\begin{aligned} \textit{State-}T_{m1} \quad & \Delta q_{T_{m1}}, V_{in}^2 = -\Delta q_{T_{m1}}^{1p1} + \Delta q_{T_{m1}}^{2p1} + \Delta q_{T_{m1}}^{2p2} + \Delta q_{T_{m1}}^{1n2} - \Delta q_{T_{m1}}^{2n1} \\ & \Delta q_{T_{m1}}, V_{po}^2 = -\Delta q_{T_{m1}}^{2p2} \\ \text{and} \quad & \Delta q_{T_{m1}}, V_{no}^2 = -\Delta q_{T_{m1}}^{2n2} \end{aligned} \tag{16}$$

$$\begin{aligned} \textit{State-}T_{m2} \quad & \Delta q_{T_{m2}}, V_{in}^2 = \Delta q_{T_{m2}}^{1p1} + \Delta q_{T_{m2}}^{1p2} + \Delta q_{T_{m2}}^{2p1} - \Delta q_{T_{m2}}^{1n1} + \Delta q_{T_{m2}}^{2n2} \\ & \Delta q_{T_{m2}}, V_{po}^2 = -\Delta q_{T_{m2}}^{1p2} \\ \text{and} \quad & \Delta q_{T_{m2}}, V_{no}^2 = -\Delta q_{T_{m2}}^{1n2} \end{aligned} \tag{17}$$

The parameters referred in (16) and (17) are that $\Delta q_{T_{mi}}, V_{in}^2$, $\Delta q_{T_{mi}}, V_{po}^2$, and $\Delta q_{T_{mi}}, V_{no}^2$ denote the differential values of electric charges in the input voltage V_{in}^2, the output voltage of the positive voltage multiplier V_{po}^2, and the output voltage of the negative voltage multiplier V_{no}^2, respectively. Therefore, the relationship between the input and output currents by substituting (16) and (17) into (7) can be stated as

$$\overline{I_{in}^2} = -4\overline{I_{out}^2} \text{ and } \overline{I_{out}^2} = \overline{I_{po}^2} = -\overline{I_{no}^2} \tag{18}$$

In (18), the turn ratio M_2 of Figure 3 is equal to 4 ($M_2 = 4$). From Figures 4(c) and 4(d), the value of the internal resistance R_{SC_2} can be expressed in terms of the consumed energies $W_{T_{m1}}$ and $W_{T_{m2}}$ as follows.

$$W_{T_m} = W_{T_{m1}} + W_{T_{m2}} = \frac{12R_d + 20R_{on}}{T_m}(\Delta q, V_{out})^2 \tag{19}$$

Thus, the internal resistance in the 2nd Section can solve from (18) and (19), which can be written as

$$R_{SC_2} = 12R_d + 20R_{on} \tag{20}$$

By combining (13) and (20), the turn ratio M and the internal resistance R_{SC} in Figure 3 can be given by

$$M = 12 \text{ and } R_{SC} = 108R_d + 20R_{on} \tag{21}$$

Therefore, the characteristics of the proposed high voltage multiplier can be stated in the K-matrix as

$$\begin{bmatrix} \overline{V_{in}} \\ \overline{I_{in}} \end{bmatrix} = \begin{bmatrix} 1/12 & 0 \\ 0 & 12 \end{bmatrix} \begin{bmatrix} 1 & 108R_d + 20R_{on} \\ 0 & 1 \end{bmatrix} \begin{bmatrix} \overline{V_{out}} \\ \overline{-I_{out}} \end{bmatrix} \tag{22}$$

In (22), the power efficiency η and the output voltage of the proposed multiplier can be rewritten as

$$\eta = \frac{R_L}{R_L + R_{SC}} = \frac{R_L}{R_L + (108R_d + 20R_{on})} \tag{23}$$

and

$$V_{out} = \left(\frac{R_L}{R_L + R_{SC}} \right) \times 12 \cdot V_{in} = \left(\frac{R_L}{R_L + (108R_d + 20R_{on})} \right) \times 12 \cdot V_{in} \tag{24}$$

4. **Simulation Results.** The performances of the proposed high voltage multiplier were studied through simulations by using the PSPICE program. The target DC output voltage was set to 3.7kV. Figure 5 shows the simulation results of the proposed multiplier by applying V_{in}= 220V@50Hz and setting T= 20μs, R_{on} = 0.1Ω, C_{pk} = C_{nl} = 10,000μF, C_{1pq} = C_{2pq} = C_{1nr} = C_{2nr} = 1μF, C_{out} = 100μF, and R_L = 1kΩ. It is seen that the output voltage of positive VMB is 1.97kV, whereas the output voltage of negative VMB is −1.73kV. The sum of these two outputs is equal to 3.7kV, which is agreed with the target output voltage. Moreover, the proposed circuit can generate the desired output of 3.7kV within 175ms. For this settling time value, the proposed high voltage multiplier thus offers high speed operation.

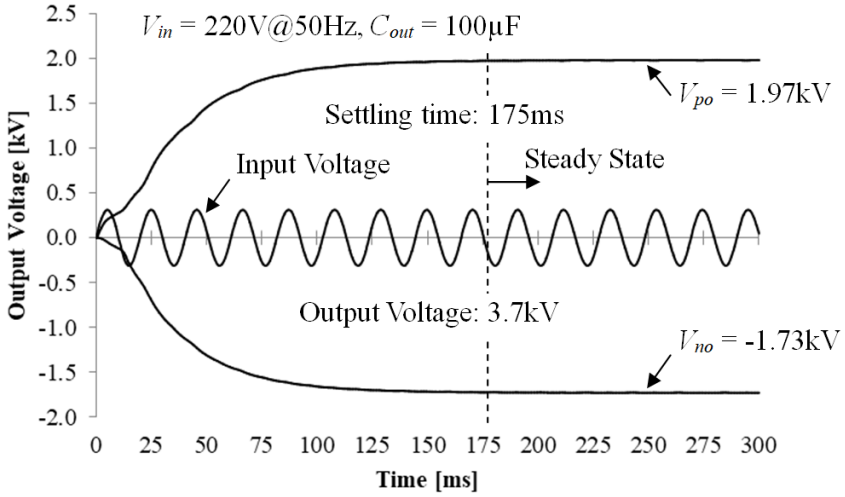

FIGURE 5. Simulation results of the proposed high voltage multiplier circuit

5. **Conclusions.** A high voltage multiplier based on switched capacitor with input voltage 220V@50Hz to generate underwater shockwaves for non-thermal food processing has been described in this paper. The validity of the circuit design has been verified by theoretical analysis. The workability of the proposed high voltage multiplier circuit has been confirmed through PSPICE simulation results. The output voltage of the proposed high voltage multiplier is suitable for further processing to turn into shockwave energy. The hardware implementation to build the non-thermal food processing for 220V@50Hz electricity is the future work.

REFERENCES

[1] M. Stoica, L. Mihalcea, D. Borda and P. Alexe, Non-thermal novel food processing technologies – An overview, *Journal of Agroalimentary Processes and Technologies*, vol.19, no.2, pp.212-217, 2013.

[2] O. Higa, R. Matsubara, K. Higa, Y. Miyafuji, T. Gushi, Y. Omine, K. Naha, K. Shimojima, H. Fukuoka, H. Maehara, S. Tanaka, T. Matsul and S. Itoh, Mechanism of the shock wave generation and energy efficiency by underwater discharge, *International Journal of Multiphysics*, vol.6, no.2, pp.89-98, 2012.

[3] S. Shinzato, Y. Higa, T. Tamaki, H. Iyama and S. Itoh, Computational simulation of underwater shock wave propagation using smoothed particle hydrodynamics, *Materials Science Forum*, vol.767, pp.86-91, 2013.

[4] H. Abe, W. Do and K. Eguchi, An efficient non-thermal food processing system by underwater shockwaves using two pairs of restoration electrodes, *Proc. of the 5th International Conference on Engineering, Applied Sciences and Technology*, pp.1-4, 2019.

[5] K. Eguchi, S. Terada and I. Oota, Design of a digitally controlled inductor-less voltage multiplier for non-thermal food processing, *International Journal of Information and Electronics Engineering*, vol.4, no.6, pp.438-445, 2014.

[6] K. Abe, H. Sasaki, I. Oota and K. Eguchi, Improvement of an output voltage efficiency of a high voltage generator for non-thermal food processing systems, *ICIC Express Letters*, vol.9, no.11, pp.3087-3092, 2015.

[7] K. Abe, I. Oota, W. Do and K. Eguchi, Synthesis of a high step-up bipolar voltage multiplier using level shift drivers, *Proc. of the 6th International Workshop on Computer Science and Engineering*, pp.305-309, 2016.

[8] K. Eguchi, A. Wongjan, A. Julsereewong, W. Do and I. Oota, Design of a high-voltage multiplier combined with Cockroft-Walton voltage multipliers and switched-capacitor ac-ac converters, *International Journal of Innovative Computing, Information and Control*, vol.13, no.3, pp.1007-1019, 2017.

[9] K. Abe, R. Ogata, K. Eguchi, K. Smerpitak and S. Pongswatd, Study on non-thermal food processing utilizing an underwater shockwave, *Indian Journal of Science and Technology*, vol.10, no.4, pp.1-5, 2017.

[10] K. Eguchi, A. Jaiwanglok, A. Julsereewong, F. Asadi, H. Abe and I. Oota, Design of a non-thermal food processing system utilizing wire discharge of dual electrodes in underwater, *International Journal of Innovative Computing, Information and Control*, vol.14, no.4, pp.847-860, 2018.

[11] S. Iqbal, A hybrid symmetrical voltage multiplier, *IEEE Trans. Power Electronics*, vol.29, no.1, pp.6-12, 2014.

[12] M. Ruzbehani, A comparative study of symmetrical Cockcroft-Walton voltage multipliers, *Journal of Electrical and Computer Engineering*, vol.2017, no.2, pp.1-10, 2017.